Deep brain stimulation re-imagined: An ultra-low frequency spike timing dependent plasticity-based approach for treating alcohol use disorder

Anders Asp
Mayo Clinic
Suelen Lucio Boschen
Mayo Clinic
Su-Youne Chang
Mayo Clinic
J. Luis Lujan (Lujan.luis@mayo.edu)
Mayo Clinic

Research Article

Keywords:

Posted Date: February 17th, 2022

DOI: https://doi.org/10.21203/rs.3.rs-1328464/v1

Abstract

Alcohol use disorder (AUD) is a chronic relapsing brain disorder characterized by an impaired ability to stop or control alcohol consumption despite adverse social, occupational, or health consequences. AUD affects nearly one-third of adults at some point during their lives, with an associated cost of approximately $249 billion annually in the U.S. alone. The effects of alcohol consumption are expected to increase significantly during the COVID-19 pandemic, with alcohol sales increased by approximately 54%, potentially exacerbating health concerns and risk-taking behaviors. Unfortunately, existing pharmacological and behavioral therapies for AUD have historically been associated with poor success rates, with approximately 40% of individuals relapsing within three years of treatment.

Pre-clinical studies have shown that chronic alcohol consumption leads to significant changes in synaptic function within the dorsal medial striatum (DMS), one of the brain regions associated with AUD and responsible for mediating goal-directed behavior. Specifically, chronic alcohol consumption has been associated with hyperactivity of dopamine receptor 1 (D1) medium spiny neurons (MSN) and hypoactivity of dopamine receptor 2 (D1) MSNs within the DMS. Optogenetic, chemogenetic, and transgenic approaches have demonstrated that reducing the D1/D2 MSN signaling imbalance decreases alcohol self-administration in rodent models of AUD.

Here, we present an electrical stimulation approach that uses ultra-low (≤ 1Hz) frequency (ULF) spike-timing dependent plasticity (STDP) in mouse models of AUD to reduce DMS D1/D2 MSN signaling imbalances by stimulating D1-MSN afferents into the GPi and ACC glutamatergic projections to the DMS in a time-locked stimulation sequence. Our data suggest that GPi/ACC ULF-STDP selectively decreases DMS D1-MSN hyperactivity leading to reduced alcohol consumption without evoking undesired affective behaviors using electrical stimulation rather than approaches requiring genetic modification. This work represents a step towards fulfilling the unmet need for a reliable method of treating severe AUD through cell-type specific control with clinically available neuromodulation tools.

Introduction

Alcohol Use Disorder (AUD) is defined as a chronic relapsing brain disorder characterized by an impaired ability to stop or control alcohol consumption despite adverse social, occupational, or health consequences [1] and is one of the most common psychiatric disorders. AUD affects nearly one-third of U.S. adults at some point during their lives and carries a financial burden greater than $249 billion annually [2]. Furthermore, it leads to approximately 88,000 preventable deaths in the U.S. each year [3]. Existent pharmacological and behavioral therapies for AUD have had poor success rates [4,5], with approximately 40% of individuals relapsing within three years of treatment [6].

It has been shown that chronic alcohol consumption leads to significant changes in glutamatergic synaptic function within the dorsal medial striatum (DMS) [7–10], one of the brain regions associated with underlying maladaptive changes observed in AUD and responsible for mediating goal-directed

behavior [11]. The DMS receives cortical glutamatergic input from limbic regions, including the medial prefrontal cortex and anterior cingulate cortex (ACC) [12,13]. The DMS contains two neuronal types: 1) Dopamine receptor 1-medium spiny neurons (D1-MSNs) and 2) Dopamine receptor 2-medium spiny neurons (D2-MSNs). D1-MSNs project to the internal Globus Pallidus (GPi) through the direct pathway and their activation results in a '*go*' signal to initiate behavior [14–18]. In contrast, D2-MSNs project to the external Globus Pallidus (GPe) through the indirect pathway and their activation serves as a '*stop*' signal to inhibit behavior [14–18]. Chronic alcohol consumption has been shown to cause permanent hyperactivity of D1-MSNs and permanent hypoactivity of D2-MSNs in the DMS via maladaptive cortical glutamatergic signaling from areas such as the ACC [7,19–22]. Studies have shown that reducing the ratio of DMS D1-MSN/D2-MSN signaling imbalance reduces pathological alcohol seeking behavior [9,10,22–30]. Furthermore, a recent report demonstrated that inducing long-term depression (LTD) by applying a single 10-minute epoch of low frequency (1Hz) optogenetic stimulation of ACC projections to the DMS, combined with systemic D1-dopamine receptor antagonism, leads to a reduction in alcohol consumption lasting for nine days [28].

Data suggest that deep brain stimulation (DBS), an increasingly prevalent therapy for motor and psychiatric disorders [31–34 35–41 42], may offer therapeutic effects for the treatment of AUD [40,41,43–46]. However, unlike DBS for movement disorders[48,49], there is an absence of reliable markers of DBS efficacy for the treatment of addiction leading to challenging selection of surgical targets and stimulation parameters. These factors, combined with nonspecific network effects of DBS [50], can lead to undesirable side effects and highly variable outcomes in the treatment of AUD and other addiction-related behaviors [39,47,51,52]. Thus, re-imagining DBS paradigms may lead to the development of new therapeutic interventions for a wide range of neuropsychiatric and neurologic disorders. Here, we leverage neuroplasticity induction protocols to selectively reverse the pathophysiology associated with the DMS D1-MSN/D2-MSN signaling imbalance underlying AUD [53–55]. Spike-timing dependent plasticity (STDP) [53–56], a natural phenomenon underlying neuroplasticity associated with learning and memory.

In STDP, bidirectional control of network gain can be achieved by repeated phase-locked activation of presynaptic and postsynaptic neural elements[56]. The direction and magnitude of the spike-timing dependent synaptic modulation is governed by the relative timing between presynaptic and postsynaptic depolarization **(Figure 1A, 1B)**. For example, long-term potentiation (LTP) is caused when postsynaptic action potentials occur repeatedly after pre-synaptic action potentials (negative timing, STDP(-)) [55,56]. On the other hand, long-term depression (LTD) is caused when post-synaptic action potentials occur repeatedly prior to pre-synaptic action potentials (positive timing, STDP(+)) [55,56] **(Figure 1C)**. Here, we describe an electrical

stimulation approach that uses ultra-low (£1Hz) frequency spike-timing dependent plasticity (ULF-STDP)[53] to reduce DMS D1/D2 MSN signaling imbalances by repeatedly stimulating the D1-MSN afferents into the GPi before stimulating ACC glutamatergic projections to the DMS **(Figure 1D)**. Action

potentials originating in D1-MSN axons within the GPi resulting from electrical stimulation will backpropagate to their somas in the DMS[57] and depolarize postsynaptic dendrites[58–60]. By leveraging the anatomical separation of D1-MSNs projections to the GPi via the direct pathway[14,61], D1-MSN axons in the GPi can be depolarized via electrical stimulation without depolarizing D2-MSN axons in the GPe. In this manner, pairing phase-locked presynaptic ACC cortical stimulation with postsynaptic GPi stimulation could provide selective control of spike-timing dependent synaptic strength in D1-MSNs while avoiding changes in synaptic strength of D2-MSNs projecting to the GPe **(Figure 2)**.

Methods

Animals: All behavior experiments were performed with wild type C57/Bl 6J mice (Jackson Laboratory, Bar Harbor, Maine, JAX Stock No: 000664). Fluorescent reporter mouse lines Drd1a-tdTomato mice (JAX Stock No: 016204) were used for labeling D1-MSNs in patch clamp electrophysiology experiments. All laboratory procedures were reviewed and approved by the Mayo Clinic Institutional Animal Care and Use Committee (IACUC) and conform to guidelines published by the NIH Guide for the Care and Use of Laboratory Animals (Department of Health and Human Services, NIH publication No. 86-23, revised 1985). Mice were housed in plastic cages under standard 12-hour light/dark cycle and conditions (21^{o}C, humidity 45%) with ad libitum access to food and water. Animals were acclimated for at least one weeks before use. All efforts were made to minimize both the number of mice used and any discomfort that may be experienced.

Stereotactic surgery: A stereotaxic frame (Model 1900, David Kopf Instruments, Tujunga, CA) was used for implantation of custom- built stimulating electrodes and Tucker-Davis Technologies (TDT) Zif-Clip microwire arrays (TDT, Alachua, FL). Custom-built stimulating electrodes consisted of bipolar 50.8 µm diameter Teflon-insulated Pt/Ir wire (A-M systems 77600, Sequim, WA) separated 200 µm apart with exposed tips cut at a 45º angle. All surgical instruments, electrodes, and skull screws were sterilized in an autoclave or MetriCide28 (Metrex, Orange, CA, USA) cold sterilant. Analgesia was provided with buprenorphine HCL (0.05 mg/kg) preoperatively and three days postoperatively. Additionally, Ibuprofen was delivered in the animals' drinking water two days prior to the surgery and no less than five days after for analgesia. Anaesthesia was induced in mice with isoflurane 4% followed by 1-2% isoflurane for maintenance. The depth of anesthesia was monitored using toe pinch and eye blink reflexes. A heating pad was used to maintain the subject's body temperature to 37.0±0.5 ºC throughout the duration of anesthesia. The surgical sites on mice heads were shaved and cleaned with betadine. Then, mice were placed in the stereotaxic apparatus and secured using ear bars. An incision of approximately 1.5 cm was made in the skin over the skull with a scalpel. Hydrogen peroxide was used to clean the skull surface. Sterile screws were used to provide a strong fixation of the head cap and serve as an electrical reference and ground. Screws were secured into 0.7mm holes drilled in the skull with a trephine drill bit. An additional craniotomy, approximately 2 mm x 2 mm in size, was created over the DMS to implant the Zif-Clip microwire array in a subset of animals. The dura was removed to expose brain tissue, which was

irrigated with cool saline throughout the surgery. For all surgical procedures, additional burr holes were drilled at the desired coordinates described next to create a cranial window for unilateral implantation of custom-built stimulating electrodes per the Mouse Brain in Stereotaxic Coordinates [12]. Stimulating electrodes were placed in the GPi (AP: -1.4 mm, ML: 1.6 mm, DV: −4.5 mm from Bregma) and ACC (AP: 0.50 mm, ML: 0.7 mm, DV: −1.85 mm from Bregma). Upon insertion and fixation of the stimulating electrodes to the skull using dental cement (Henry Schein, Melville, NY), a Zif-Clip microwire array was chronically implanted into the DMS (array center: AP: 0.70 mm, ML: 1.5 mm, DV: −2.75 mm from Bregma). Kwik-Sil silicone elastomer (World Precision Instruments, Sarasota, FL, USA) was put around the Zif-Clip microwire array and stimulating electrodes to maintain a seal between the brain and dental cement described in the next step. Finally, all components were secured with Metabond dental cement (Parkell, Edgewood, NY, USA). After the electrode implantation surgery, the animals were housed individually for one week to allow sufficient time for recovery. Animals were monitored twice daily for five days following surgery for signs of distress and infection at the surgical site. If signs of infection or distress were observed, topical polysporin antibacterial ointment was applied to the surgical site or a veterinarian was consulted for the appropriate methods of treatment. Animals were excluded from behavioral and electrophysiological analysis if they demonstrated weight loss greater than or equal to 20% body weight if they demonstrated inability to ambulate or were unable access food and water as a result of surgical procedures. Additionally, animals were excluded upon mechanical failure of dental cement headcap or chronically implanted electrodes.

Electrical stimulation parameters: Electrical stimulation was delivered through custom-built bipolar parallel chronically indwelling stimulating electrodes via a IZ2M-64 microstimulator programmed in the Synapse software (TDT, Alachua, FL). The ultra-low frequency spike-timing dependent plasticity stimulation (ULF-STDP) protocol consists of a charge-balanced, biphasic, cathodic-leading, 250 µA current stimulation with a pulse duration of 90µs delivered to the GPi and ACC with 18ms between GPi and ACC stimulation. GPi-ACC stimulation pairing was delivered at 1Hz for 10 minutes. ULF-STDP(+) is defined as postsynaptic GPi stimulation 18 ms prior to presynaptic ACC stimulation and ULF-STDP(-) is defined as presynaptic ACC stimulation 18 ms prior to postsynaptic GP stimulation. Current was delivered at a density of 941 µC/cm^2 such that Shannon safety criteria are satisfied to avoid tissue damage[13].

Two-bottle choice alcohol self-administration AUD model: A standard two-bottle choice paradigm was used to assess alcohol consumption and preference[62]. Briefly, animals were implanted with stimulating electrodes as described in the *Stereotactic Surgery* section and allowed one week for recovery. Two bottles were presented daily in the animal's home cages: one containing water and the other alcohol [63] at the onset of the dark cycle. Bottles consisted of a Hydropac valve (Avidity Science, Waterford, WI, USA) affixed the cap to a 50mL falcon conical tube (Corning, Corning, NY, USA). The position of the alcohol and water bottles was swapped daily to reduce confounds produced by location preference. For the first week, alcohol concentrations were increased every other day from 3% to 6% to 10% v/v. For the remaining duration of the experiment, mice were presented with one bottle of water and another bottle with 10%

alcohol. For three alcohol exposure days prior to ULF-STDP stimulation, the animals were tethered to the stimulating system to allow habituation to the procedure. At day 25, animals were stimulated with the ULF-STDP protocol described in the methods section under *Electrical stimulation parameters* if mean and standard error of alcohol consumption (calculated in g/kg of body mass at be beginning of the night cycle) was less than 20% over a 3-day period after at least two weeks of alcohol exposure. The mass of each mouse, the mass of alcohol consumed, and the mass of water consumed was assessed daily using a scale. Additionally, an IR beam break sensor was placed in front of the sippers to measure the total time spent interacting with the sipper. Data were analyzed and plotted using Prism v9 software (GraphPad, San Diego, CA)

Limited-access AUD model: A limited access model of AUD capable of achieving blood alcohol content >1mg/ml in mice was used to assess acute alcohol consumption [64]. Briefly, animals were implanted with stimulating and recording electrodes as described in the *Stereotactic Surgery* section and allowed one week for recovery. Mice were then provided with daily 2-hour access of 20% v/v ethanol in their home cages beginning three hours after the onset of the dark cycle for ten days. Immediately prior to providing alcohol on day ten, animals were stimulated with the ULF-STDP(+) protocol described in the methods section under *Electrical stimulation parameters*. For three alcohol exposure days prior to ULF-STDP(+) stimulation, the animals were tethered to the stimulating and recording system to allow habituation to the handling procedure. The mass of each mouse, the mass of alcohol consumed, and the mass of water consumed was assessed daily using a scale. Data were analyzed and plotted using Prism v9 software (GraphPad, San Diego, CA)

In vivo electrophysiology: Previously described standard methods were followed for *in vivo* electrophysiological recordings of MSNs within the DMS [59]. Briefly, mice were surgically implanted with chronic indwelling Pt/Ir stimulating electrodes in the GPi and ACC along with a TDT 32-channel ZIF-Clip microwire array (TDT, Alachua, FL) placed in the DMS as described in the *Stereotactic Surgery* section. Mice were allowed one week to recover from surgery prior to recordings during unrestrained locomotion. Electrophysiological recordings were performed in three stages: alcohol naïve, following repeated alcohol exposure in the *Limited Access AUD model*, and following ULF-STDP stimulation. Multichannel extracellular recordings were performed at 50 kHz and band-pass filtered from 300 Hz to 5 kHz prior to spike thresholding and sorted using principal component analysis (PCA) via the TDT Synapse software (TDT, Alachua, FL). Mean event rates over 10-minute periods were compared immediately before and after ULF-STDP application using MATLAB (MathWorks, Inc., Natick, MA) Student's unpaired t-test ($p<0.05$), Data were plotted using Prism v9 software (GraphPad, San Diego, CA). Additionally, extracellular LFPs band-pass filtered from 1-300 Hz were recorded from chronically implanted electrodes. Power spectral density of the GPi, DMS, and ACC was be analyzed following previously described methods[65] across delta (1-4 Hz), theta (4-8 Hz), alpha (8-12 Hz), beta (13-30 Hz), and gamma (31-70 Hz) bands.

***Ex vivo* whole-cell patch clamp electrophysiology:** We followed standard procedures for slice preparation and *ex vivo* whole cell electrophysiology to measure D1-MSN activity [10,66,67]. Five week-old alcohol-naiive Drd1a-tdTomato mice (JAX Stock No: 016204) were assigned randomly to receive either ULF-STDP(+)

in vivo or sham surgery while under 1-2% isoflurane anesthesisia 30 minutes prior to euthanasia for whole cell patch clamp electrophysiology experiments. Briefly, cells were clamped at -75 mV in the presence of lidocaine (0.7 mM) to record spontaneous mEPSCs. The mEPSC amplitude and frequency were compared between animals which received ULF-STDP(+) and stimulation naiive animals. Statistical significance ($p<0.05$) was determined via unpaired Student's t-tests using MATLAB (MathWorks, Inc., Natick, MA). Data were plotted using Prism v9 software (GraphPad, San Diego, CA). D1-MSNs were identified by fluorescence microscopy in Drd1a-tdTomato mice.

Euthanasia and Histology: At the end of the experiments, animals were euthanized by a lethal overdose of Pentobarbital (i.p.), in accordance with the Panel on Euthanasia of the American Veterinary Medical Association (A.V.M.A.). Mice were transcardially perfused with 4% paraformaldehyde in phosphate buffered saline (PBS). Mice brains were removed and dehydrated in 30% sucrose prior to flash-freezing with dry ice and slicing into 40 µm-thick coronal sections using a sliding microtome (Leica Biosystems, Buffalo Grove, IL). Slices were mounted and counterstained with DAPI (Vector Laboratories, Burlingame, CA, USA) and visualized using bright field and fluorescence microscopy (Carl Zeiss LSM780 or Nikon Eclipse FN1) to verify electrode location. Animals were included in behavioral and electrophysiological analysis only if at least one of each bipolar electrode tips were located in both the ACC and GPi as defined by atlas boundaries.[12] Animals with electrodes absent in the ACC and GPi were excluded from all behavioral and electrophysiological analysis.

Rigor and reproducibility: The observed effect size of ULF-STDP in reducing alcohol consumption was $d_{Cohen} = 0.603$, in which 75% of the mice (15 out of 20 mice) developed high alcohol preference in the two-bottle choice model of AUD. Animal numbers for each cohort in each behavioral experiment were determined based on an 80% statistical power, 95% confidence interval, and effect size of 0.603. Experimenters were blinded to stimulation parameters during allocation, data collection, and data analysis. Data collected were tested for normality with the Kolmogorov-Smirnov test. Comparisons of non-normal distributions were performed using nonparametric tests, substituting the Mann-Whitney U-test in place of the unpaired Student's t-test.

Results

ULF-STDP allows bidirectional control of alcohol consumption in a two-bottle choice model of AUD. Our initial goal was to determine if ULF-STDP(+) decreases alcohol consumption in a two-bottle choice mouse model of AUD. Mice implanted with stimulating electrodes in the ACC and GPi reached stable consumption of 10% v/v alcohol and were separated into two groups, a high alcohol preference group defined as >60% preference and low alcohol preference group defined as <60% preference **(Figure 3A)**. ULF-STDP(+) reduced alcohol consumption in the high alcohol preference group with a decrease of 3.2 g/kg/24hr in the mean of differences ($n=15$, $p<0.05$) **(Figures 3A, B)**. Conversely, ULF-STDP(-) increased alcohol consumption in the low alcohol preference group with an increase of 5.2 g/kg/24hr in the mean of differences ($n=5$, $p<0.05$) **(Figures 3A, C)**. ULF-STDP(+) did not affect food **(Figure 3D)** or water **(Figure 3E)** consumption in a random subset of the high alcohol preference group ($n=5$, $p<0.05$). ULF-STDP(+)

reduced time drinking alcohol for 170 minutes **(Figure 3F)**, but this effect was absent 360-490 minutes after stimulation **(Figure 3G)**, suggesting that reductions in alcohol consumption may be transient. Importantly, alcohol consumption in the two-bottle choice model was not affected when the ULF-STDP(+) protocol was applied to only the ACC or GPi electrode (**Figure S1).**

ULF-STDP(+) reduces DMS mean firing rate.Our next goal was to characterize if ULF-STDP(+) alters DMS MSN firing patterns underlying behavioral changes. Single unit potentials in the DMS were recorded from chronically indwelling microwire arrays (Figure 4A, B) in high alcohol preference mice before and after ULF-STDP (+). MSNs **(Figure 4C, left)** were distinct and separable from non-MSN units **(Figure 4C, right)** in the DMS, as determined by PCA. Only units identified as MSN were included in firing rate calculations. A reduction in MSN firing rate is evident in the representative DMS microwire array channel of a high alcohol preference animal before **(Figure 4D, top)** and after **(Figure 4D, bottom)** ULF-STDP(+). The median MSN firing rate calculated over a two-hour period was reduced from 0.17Hz to 0.08Hz after ULF-STDP(+) **(Figure 4E)** (n=116 cells, n=4 mice, p=0.0001). Of the 116 units, 17.24% showed an increase in mean firing rate,73.28% showed a decrease in mean firing rate, and 9.48% of units showed no change mean firing rate before and after ULF-STDP(+) **(Figure 4F)**. Alcohol consumption was also monitored in the chronic intermittent access model of AUD. After nine days of stable alcohol consumption, ULF-STDP(+) was delivered immediately prior to alcohol presentation on day 10, resulting in a decrease of 2.54 g/kg/2hr in the mean of differences (n=4, p<0.05) **(Figure 4G,H).** Microwire array impedances were stable over the course of the experiment **(Figure S2)**. Additionally, there were no differences in spectral band power before and after ULF-STDP(+) **(Figure S3)**.

ULF-STDP(+) reduces evoked multiunit potentials in the DMS in vivo. The mechanism of action of ULF-STDP for reducing alcohol consumption is predicated on altering the strength of synaptic connections between the cortex and striatum. Therefore, we tested if ULF-STDP(+) specifically reduced evoked corticostriatal multiunit potentials in the DMS of anesthetized mice. Multiunit potentials in the DMS can be evoked by GPi **(Figure 5A)** and ACC stimulation **(Figure 5B)**. ULF-STDP(+) reduced the peak evoked multiunit potential from ACC stimulation with a mean of differences of 17.97μV, but no change was observed in responses evoked by GPi stimulation **(Figure 5C)** (n=21 channels from 3 mice, p<0.05). Stimulation to peak evoked multiunit response latency did not differ across stimulation locations and was not affected by ULF-STDP(+) **(Figure 5D)**.

ULF-STDP(+) reduces DMS D1-MSN synaptic strength ex vivo. D1-MSNs in the DMS show increased glutamatergic transmission after chronic exposure to alcohol [7,19–22]. Reducing the synaptic strength of DMS D1-MSNs also reduces alcohol consumption [9]. Therefore, we tested if ULF-STDP(+) reduces synaptic strength of DMS D1-MSNs by comparing *ex vivo* D1-MSN miniature excitatory postsynaptic current (mEPSC) amplitude and frequency in the DMS from stimulation-naïve animals to those that received ULF-STDP(+) *in vivo.* Representative DMS D1-MSN whole cell voltage clamp current traces from stimulation-naiive animals and those that received ULF-STDP(+) were identified with a positive Td-Tomato reporter **(Figure 6A)**. ULF-STDP(+) decreased D1-MSN mEPSC amplitude **(Figures 6B, C)**, but not frequency **(Figure 6D, E)** (n=3 cells from 1 ULF-STDP(+) mouse; n=7 cells from 5 naiive mice, p<0.05).

Discussion

Here, we describe a novel approach for using spike-timing dependent plasticity (STDP) to reverse maladaptive hyperactivity of DMS D1-MSNs associated with increased alcohol consumption in alcohol use disorder (AUD). This approach relies upon a method of delivering paired electrical pulses through multiple electrodes at an ultra-low (≤1Hz) frequency (ULF) to induce STDP onto D1-MSNs in the direct pathway. The results described here are consistent with an emerging body of literature suggesting that reducing alcohol-associated D1-MSN hyperactivity or increasing D2-MSN hypoactivity reduces alcohol seeking and consumption [9,10,22–30]. We tested the hypothesis that GPi/ACC ULF-STDP(+) will selectively decrease alcohol consumption and D1-MSN synaptic strength in a mouse model of AUD **(Figure 7)**. By applying ULF-STDP stimulation to the ACC and GPi, we demonstrate selective bidirectional gain control of glutamatergic ACC efferents to D1-MSNs of the direct pathway **(Figure 3A).** These findings are consistent with the hypothesis that repeated phase-locked stimulation of the presynaptic axons in the cingulum bundle projecting from the ACC and the postsynaptic D1-MSN axons projecting to the GPi may avoid plasticity induction in D2-MSNs, which project to the GPe and may limit plasticity induction in other spatially distant brain regions.

While the alcohol-specific effects of ULF-STDP(+) are promising, care must be taken not to induce hypoactivity of the direct pathway, as undesirable reductions in general locomotor activity[62] and goal directed behavior[63] have been reported. Our data show that ULF-STDP(+) decreases alcohol consumption without influencing food or water consumption**(Figure 3D,E)**, suggesting that ULF-STDP(+) does not interfere with general consummatory behavior. Additionally, ULF-STDP(+) delivered in a real-time place preference task does not alter distance traveled, but it does decrease velocity and increase time spent in the zone paired with ULF-STDP(+) **(Figure S4).** Further studies must be conducted to optimize ULF-STDP(+) dosing and re-dosing parameters (e.g., stimulation interval, stimulation conditions, etc.) in such a manner that ULF-STDP(+) maximizes reductions in alcohol consumption without negatively affecting general motor or reward-related behavior.

Assessment of neurological function at the single cell and neural circuit levels is paramount to establish a causal functional role of a synaptic neuroplasticity induction protocol such as ULF-STDP in altering neural network function, and ultimately influencing behavior. We demonstrated that reduction in alcohol consumption mediated by ULF-STDP(+) is accompanied by neurological adaptations *in vivo.* Specifically, we show that ULF-STDP(+) causes a reduction in the mean firing rate of DMS-MSNs and a reduction in alcohol consumption **(Figure 4)**. This association between *in vivo* DMS-MSN firing rate and reduction in alcohol consumption is consistent with other reports using a D1 receptor antagonist to reduce DMS-MSN firing rate and alcohol consumption[68]. This decrease in firing rate is likely driven by D1-MSNs. However, the *in vivo* electrophysiology single unit recordings performed here do not allow for the determination of firing rate changes across different cell-types. Thus, future studies using cell-specific optical interfacing approaches such as *in vivo* calcium imaging may allow for a more comprehensive analysis of cell types affected by ULF-STDP.

The strength of the ACC-DMS-GPi circuit is positively correlated with behaviors associated with AUD. For ULF-STDP to engage this ACC-DMS-GPi circuit and reverse maladaptive neuroplasticity associated with AUD, numerous criteria must be satisfied. Pre and post synaptic elements consisting of ACC projection neurons and D1-MSNs, respectively, must be repeatedly activated with a phase offset of approximately 18ms between electrodes. Additionally, ULF-STDP requires precise target selection such that action potentials originating in the GPi and ACC propagate to the DMS. To confirm functional engagement of the ACC-DMS-GPi circuit *in vivo*, we demonstrate stimulation originating in the ACC travels orthodromically to evoke multiunit potentials in the DMS and that stimulation originating in the GPi generates antidromically traveling multiunit potentials detectable in the DMS **(Figure 5)**. Additionally, the 1ms latency to peak evoked potential in the DMS **(Figure 5)** is consistent with delays due to action potential propagation rates of a monosynaptic connection[69]. Furthermore, we demonstrated that ULF-STDP(+) decreased peak potentials evoked by ACC stimulation, but not by GPi stimulation **(Figure 5).** These findings show that ULF-STDP(+) decreases the strength of ACC-DMS synapses without altering the antidromic responses from GPi stimulation in an intact ACC-DMS-GPi circuit, indicating successful functional target engagement.

Multiple factors influence the direction and magnitude of neuroplasticity induced by STDP, including the relative timing of presynaptic and postsynaptic depolarizations, the number of pulse pairings, the cell types involved in the synapse, behavioral contexts, and extracellular levels of neuromodulators such as dopamine. Here we demonstrated that ULF-STDP(+) applied *in vivo* to the ACC and GPi decreases D1-MSN mEPSC amplitude, but not the mEPSC inter event interval, in a whole cell *ex vivo* mouse brain slice preparation **(Figure 6)**. These findings are consistent with initial investigations into the mechanisms and effects of STDP performed in cultured hippocampal cells showing repetitive postsynaptic spiking approximately 20 msec before presynaptic activation resulted in LTD[56].This study also demonstrated that reversing the relative timing between the pre and postsynaptic activation leads to LTP [56]. Additional studies showed that both LTP and LTD can occur in corticostriatal synapses with similar pre-post activation timings [70]. Conversely, it has also been demonstrated that in corticostriatal synapses, presynaptic depolarization prior to postsynaptic depolarization causes LTD [71,72]. While our findings may appear to disagree with prior studies, there are important methodological differences that explain these seemingly contradictory results. Namely, ULF-STDP is delivered while the animal is awake and during a state of acute withdrawal **(Figures 3, 4)**. Acute withdrawal is associated with a decrease in extracellular dopamine [73,74], which biases STDP to produce LTD in D1-MSNs and LTP in D2-MSNs regardless of whether a pre- or post-synaptic action potential occurs first [55]. Additionally, it is important to note that the direct and indirect pathways are largely but not entirely comprised of D1-MSNs and D2-MSNs, respectively [75] Furthermore, the exact contribution of D2-MSNs projecting to the GPi remains unknown. To avoid the theoretical risk of de-potentiating D2-MSNs projecting to the GPi, we delivered the postsynaptic stimulation prior to the presynaptic stimulation. Additional studies to characterize the synaptic effects of ULF-STDP on both D1-MSNs and D2-MSNs with varying stimulation parameters and pharmacological control experiments must be performed to fully determine the cell-type specificity and confirm the effects of ULF-STDP are restricted to the direct pathway. For example, STDP in the ACC-DMS-

GPi circuit is suspected to be dependent on CB-1 endocannabinoid receptor (CB1R) activation[54,55,76]. To test if synaptic strength changes mediated by ULF-STDP(+) are dependent on a classical STDP mechanism dependent on CB1R activation future studies should investigate how CB1R pharmacological manipulation influences electrophysiological and behavioral outcomes of ULF-STDP(+).

There are distinct advantages to move away from traditional high frequency DBS toward pulse sequences designed to treat maladaptive neuroplasticity. First among these advantages is enhanced control of specific cell types and circuits. Others have previously employed DBS to enable cell-specific reversal of drug-related maladaptive striatal plasticity [77,78]. However, our approach enables control of synaptic strength of specific cell types without pharmacological modulation or genetic modification through the selection of electrode placement that enables strategic stimulation of pre and post synaptic neural elements to alter synaptic strength and behavior. Reliance on electrical stimulation alone is paramount, as it obviates problems associated with clinical adoption of genetic manipulation required for approaches such as optogenetics and chemogenetics while avoiding undesirable off-target effects of pharmacological tools like D1-dopamine receptor antagonists[79]. Furthermore, this study represents a new direction for clinical therapies like DBS by enabling correction of dysfunction associated with maladaptive neuroplasticity rather than acutely treating symptoms. Additionally, the energy required for an ultra-low frequency (≤1 Hz) neuromodulation protocol is over two orders of magnitude lower than that of an equivalent waveform delivered at a high frequency (~130 Hz) according to Rayleigh's energy theorem[80]. While ULF-STDP(+) is in a very early pre-clinical stage and is NOT ready for clinical use, lowering power consumption will eventually lead to improved battery life, reducing the frequency of battery recharging cycles and surgical replacement procedures.

ULF-STDP allows for network-level gain control in deep brain structures previously unachievable with existing clinical neuromodulation approaches. Taken together, our results suggest that novel neuromodulation approaches such as the one described herein, which is based on reversing maladaptive neuroplasticity underlying symptom-specific circuitopathies, may improve the capabilities of existing invasive neuromodulation therapies and allow for expansion to new indications. In turn, this may enable a new class of neuromodulation therapies for treatment of a wide range of disorders associated with maladaptive plasticity of the cortico-striato-pallidal pathway beyond AUD such as Tourette's syndrome [81], Obsessive Compulsive Disorder (OCD) [82,83], Schizophrenia [84], Parkinson's Disease (PD) [85–87], Manic Depression [88], Exploring novel spatiotemporally structured simulation of brain structures beyond the cortico-striato-pallidal circuit may enable long-lasting reductions in symptoms and reduce off-target effects for both existing and new neurological indications.

Declarations

Author contributions statement:

AA wrote the main manuscript text. AA, SB, SC, and JL made significant contributions to the conception and design of the work. AA performed all data acquisition, analysis, and figure preparation. AA, SB, SC,

and JL interpreted the data. All authors have reviewed and approved the manuscript. Furthermore, all authors have agreed to be personally accountable for the author's own contributions.

Ethics statement:

The author(s) declare no competing interests. This study is reported in accordance with ARRIVE guidelines

Data availability statement:

All datasets and code necessary to interpret, verify, and extend research in the article will be provided by corresponding author upon request.

References

1. Alcohol Use Disorder. *Natl. Inst. Alcohol Abuse Alcohol. NIAAA* (2011). at <https://www.niaaa.nih.gov/alcohol-health/overview-alcohol-consumption/alcohol-use-disorders>
2. Sacks, J. J., Gonzales, K. R., Bouchery, E. E., Tomedi, L. E. & Brewer, R. D. 2010 National and State Costs of Excessive Alcohol Consumption. *Am. J. Prev. Med.* **49**<bvertical-align:super;>,</bvertical-align:super;> e73–e79 (2015).
3. Alcohol Facts and Statistics. *Natl. Inst. Alcohol Abuse Alcohol. NIAAA* (2019). at <https://www.niaaa.nih.gov/publications/brochures-and-fact-sheets/alcohol-facts-and-statistics>
4. Swift, R. M. & Aston, E. R. Pharmacotherapy for Alcohol Use Disorder: Current and Emerging Therapies. *Harv. Rev. Psychiatry* **23**<bvertical-align:super;>,</bvertical-align:super;> 122–133 (2015).
5. Becker, H. C. Alcohol Dependence, Withdrawal, and Relapse. *Alcohol Res. Health* **31**<bvertical-align:super;>,</bvertical-align:super;> 348–361 (2008).
6. Moos, R. H. & Moos, B. S. Rates and predictors of relapse after natural and treated remission from alcohol use disorders. *Addict. Abingdon Engl.* **101**<bvertical-align:super;>,</bvertical-align:super;> 212–222 (2006).
7. Wang, J., Cheng, Y., Wang, X., Hellard, E. R., Ma, T., Gil, H., Hamida, S. B. & Ron, D. Alcohol Elicits Functional and Structural Plasticity Selectively in Dopamine D1 Receptor-Expressing Neurons of the Dorsomedial Striatum. *J. Neurosci.* **35**<bvertical-align:super;>,</bvertical-align:super;> 11634–11643 (2015).
8. Everitt, B. J. & Robbins, T. W. Drug Addiction: Updating Actions to Habits to Compulsions Ten Years On. *Annu. Rev. Psychol.* **67**<bvertical-align:super;>,</bvertical-align:super;> 23–50 (2016).
9. Cheng, Y., Huang, C. C. Y., Ma, T., Wei, X., Wang, X., Lu, J. & Wang, J. Distinct Synaptic Strengthening of the Striatal Direct and Indirect Pathways Drives Alcohol Consumption. *Biol. Psychiatry* **81**<bvertical-align:super;>,</bvertical-align:super;> 918–929 (2017).
10. Ma, T., Cheng, Y., Hellard, E. R., Wang, X., Lu, J., Gao, X., Huang, C. C. Y., Wei, X.-Y., Ji, J.-Y. & Wang, J. Bidirectional and long-lasting control of alcohol-seeking behavior by corticostriatal LTP and LTD. *Nat. Neurosci.* **21**<bvertical-align:super;>,</bvertical-align:super;> 373 (2018).

11. Balleine, B. W., Delgado, M. R. & Hikosaka, O. The Role of the Dorsal Striatum in Reward and Decision-Making. *J. Neurosci.* **27**<bvertical-align:super;>,</bvertical-align:super;> 8161–8165 (2007).
12. Koob, G. F. & Volkow, N. D. Neurocircuitry of addiction. *Neuropsychopharmacol. Off. Publ. Am. Coll. Neuropsychopharmacol.* **35**<bvertical-align:super;>,</bvertical-align:super;> 217–238 (2010).
13. Koob, G. F. & Volkow, N. D. Neurobiology of addiction: a neurocircuitry analysis. *Lancet Psychiatry* **3**<bvertical-align:super;>,</bvertical-align:super;> 760–773 (2016).
14. Gerfen, C. R. & Surmeier, D. J. Modulation of striatal projection systems by dopamine. *Annu. Rev. Neurosci.* **34**<bvertical-align:super;>,</bvertical-align:super;> 441–466 (2011).
15. Deniau, J. M. & Chevalier, G. The lamellar organization of the rat substantia nigra pars reticulata: distribution of projection neurons. *Neuroscience* **46**<bvertical-align:super;>,</bvertical-align:super;> 361–377 (1992).
16. Albin, R. L., Young, A. B. & Penney, J. B. The functional anatomy of basal ganglia disorders. *Trends Neurosci.* **12**<bvertical-align:super;>,</bvertical-align:super;> 366–375 (1989).
17. Gerfen, C. R., Staines, W. A., Arbuthnott, G. W. & Fibiger, H. C. Crossed connections of the substantia nigra in the rat. *J. Comp. Neurol.* **207**<bvertical-align:super;>,</bvertical-align:super;> 283–303 (1982).
18. Calabresi, P., Picconi, B., Tozzi, A., Ghiglieri, V. & Di Filippo, M. Direct and indirect pathways of basal ganglia: a critical reappraisal. *Nat. Neurosci.* **17**<bvertical-align:super;>,</bvertical-align:super;> 1022–1030 (2014).
19. Stefanini, E., Frau, M., Garau, M. G., Garau, B., Fadda, F. & Gessa, G. L. Alcohol-preferring rats have fewer dopamine D2 receptors in the limbic system. *Alcohol Alcohol. Oxf. Oxfs.* **27**<bvertical-align:super;>,</bvertical-align:super;> 127–130 (1992).
20. McBride, W. J., Chernet, E., Dyr, W., Lumeng, L. & Li, T. K. Densities of dopamine D2 receptors are reduced in CNS regions of alcohol-preferring P rats. *Alcohol Fayettev. N* **10**<bvertical-align:super;>,</bvertical-align:super;> 387–390 (1993).
21. Volkow, N. D., Wang, G. J., Fowler, J. S., Logan, J., Hitzemann, R., Ding, Y. S., Pappas, N., Shea, C. & Piscani, K. Decreases in dopamine receptors but not in dopamine transporters in alcoholics. *Alcohol. Clin. Exp. Res.* **20**<bvertical-align:super;>,</bvertical-align:super;> 1594–1598 (1996).
22. Robins, M. T., Chiang, T., Mores, K. L., Alongkronrusmee, D. & van Rijn, R. M. Critical Role for Gi/o-Protein Activity in the Dorsal Striatum in the Reduction of Voluntary Alcohol Intake in C57Bl/6 Mice. *Front. Psychiatry* **9**<bvertical-align:super;>,</bvertical-align:super;> (2018).
23. D'Souza, M. S., Ikegami, A., Olsen, C. M. & Duvauchelle, C. L. Chronic D1 agonist and ethanol coadministration facilitate ethanol-mediated behaviors. *Pharmacol. Biochem. Behav.* **76**<bvertical-align:super;>,</bvertical-align:super;> 335–342 (2003).
24. El-Ghundi, M., George, S. R., Drago, J., Fletcher, P. J., Fan, T., Nguyen, T., Liu, C., Sibley, D. R., Westphal, H. & O'Dowd, B. F. Disruption of dopamine D1 receptor gene expression attenuates alcohol-seeking behavior. *Eur. J. Pharmacol.* **353**<bvertical-align:super;>,</bvertical-align:super;> 149–158 (1998).

25. Thanos, P. K., Volkow, N. D., Freimuth, P., Umegaki, H., Ikari, H., Roth, G., Ingram, D. K. & Hitzemann, R. Overexpression of dopamine D2 receptors reduces alcohol self-administration. *J. Neurochem.* **78**<bvertical-align:super;>,</bvertical-align:super;> 1094–1103 (2001).
26. Phillips, T. J., Brown, K. J., Burkhart-Kasch, S., Wenger, C. D., Kelly, M. A., Rubinstein, M., Grandy, D. K. & Low, M. J. Alcohol preference and sensitivity are markedly reduced in mice lacking dopamine D 2 receptors. *Nat. Neurosci.* **1**<bvertical-align:super;>,</bvertical-align:super;> 610–615 (1998).
27. Dyr, W., McBride, W. J., Lumeng, L., Li, T.-K. & Murphy, J. M. Effects of D1 and D2 dopamine receptor agents on ethanol consumption in the high-alcohol-drinking (HAD) line of rats. *Alcohol* **10**<bvertical-align:super;>,</bvertical-align:super;> 207–212 (1993).
28. Roltsch Hellard, E., Binette, A., Zhuang, X., Lu, J., Ma, T., Jones, B., Williams, E., Jayavelu, S. & Wang, J. Optogenetic control of alcohol-seeking behavior via the dorsomedial striatal circuit. *Neuropharmacology* **155**<bvertical-align:super;>,</bvertical-align:super;> 89–97 (2019).
29. Hong, S.-I., Kang, S., Chen, J.-F. & Choi, D.-S. Indirect medium spiny neurons in the dorsomedial striatum regulate ethanol-containing conditioned reward seeking. *J. Neurosci.* 0876–19 (2019). doi:10.1523/JNEUROSCI.0876-19.2019
30. Cheng, Y. & Wang, J. The use of chemogenetic approaches in alcohol use disorder research and treatment. *Alcohol* **74**<bvertical-align:super;>,</bvertical-align:super;> 39–45 (2019).
31. Deep-Brain Stimulation for Parkinson's Disease Study Group, Obeso, J. A., Olanow, C. W., Rodriguez-Oroz, M. C., Krack, P., Kumar, R. & Lang, A. E. Deep-brain stimulation of the subthalamic nucleus or the pars interna of the globus pallidus in Parkinson's disease. *N. Engl. J. Med.* **345**<bvertical-align:super;>,</bvertical-align:super;> 956–963 (2001).
32. Flora, E. D., Perera, C. L., Cameron, A. L. & Maddern, G. J. Deep brain stimulation for essential tremor: a systematic review. *Mov. Disord. Off. J. Mov. Disord. Soc.* **25**<bvertical-align:super;>,</bvertical-align:super;> 1550–1559 (2010).
33. Krauss, J. K. Deep brain stimulation for dystonia in adults. Overview and developments. *Stereotact. Funct. Neurosurg.* **78**<bvertical-align:super;>,</bvertical-align:super;> 168–182 (2002).
34. Wu, C. & Sharan, A. D. Neurostimulation for the treatment of epilepsy: a review of current surgical interventions. *Neuromodulation J. Int. Neuromodulation Soc.* **16**<bvertical-align:super;>,</bvertical-align:super;> 10–24; discussion 24 (2013).
35. Anderson, R. J., Frye, M. A., Abulseoud, O. A., Lee, K. H., McGillivray, J. A., Berk, M. & Tye, S. J. Deep brain stimulation for treatment-resistant depression: Efficacy, safety and mechanisms of action. *Neurosci. Biobehav. Rev.* **36**<bvertical-align:super;>,</bvertical-align:super;> 1920–1933 (2012).
36. Bittar, R. G., Kar-Purkayastha, I., Owen, S. L., Bear, R. E., Green, A., Wang, S. & Aziz, T. Z. Deep brain stimulation for pain relief: a meta-analysis. *J. Clin. Neurosci. Off. J. Neurosurg. Soc. Australas.* **12**<bvertical-align:super;>,</bvertical-align:super;> 515–519 (2005).
37. Halpern, C. H., Wolf, J. A., Bale, T. L., Stunkard, A. J., Danish, S. F., Grossman, M., Jaggi, J. L., Grady, M. S. & Baltuch, G. H. Deep brain stimulation in the treatment of obesity. *J. Neurosurg.* **109**<bvertical-align:super;>,</bvertical-align:super;> 625–634 (2008).

38. Deep brain stimulation in 18 patients with severe Gilles de la Tourette syndrome refractory to treatment: the surgery and stimulation | Journal of Neurology, Neurosurgery & Psychiatry. at <http://jnnp.bmj.com/content/79/2/136.short>
39. Luigjes, J., Brink, W. van den, Feenstra, M., Munckhof, P. van den, Schuurman, P. R., Schippers, R., Mazaheri, A., Vries, T. J. D. & Denys, D. Deep brain stimulation in addiction: a review of potential brain targets. *Mol. Psychiatry* **17**<bvertical-align:super;>,</bvertical-align:super;> 572–583 (2012).
40. Kuhn, J., Lenartz, D., Huff, W., Lee, S., Koulousakis, A., Klosterkoetter, J. & Sturm, V. Remission of alcohol dependency following deep brain stimulation of the nucleus accumbens: valuable therapeutic implications? *J. Neurol. Neurosurg. Psychiatry* **78**<bvertical-align:super;>,</bvertical-align:super;> 1152–1153 (2007).
41. Müller, U. J., Sturm, V., Voges, J., Heinze, H.-J., Galazky, I., Heldmann, M., Scheich, H. & Bogerts, B. Successful treatment of chronic resistant alcoholism by deep brain stimulation of nucleus accumbens: first experience with three cases. *Pharmacopsychiatry* **42**<bvertical-align:super;>,</bvertical-align:super;> 288–291 (2009).
42. Okun, M. S. The Transition of Deep Brain Stimulation from Disease Specific to Symptom Specific Indications. *Rinsho Shinkeigaku* **52**<bvertical-align:super;>,</bvertical-align:super;> 891–895 (2012).
43. Voges, J., Müller, U., Bogerts, B., Münte, T. & Heinze, H.-J. Deep Brain Stimulation Surgery for Alcohol Addiction. *World Neurosurg.* <bvertical-align:super;>80</bvertical-align:super;><bvertical-align:super;>,</bvertical-align:super;> S28.e21-S28.e31 (2013).
44. Heinze, H.-J., Heldmann, M., Voges, J., Hinrichs, H., Marco-Pallares, J., Hopf, J.-M., Müller, U., Galazky, I., Sturm, V., Bogerts, B. & Münte, T. F. Counteracting incentive sensitization in severe alcohol dependence using deep brain stimulation of the nucleus accumbens: clinical and basic science aspects. *Front. Hum. Neurosci.* **3**<bvertical-align:super;>,</bvertical-align:super;> (2009).
45. Pelloux, Y., Degoulet, M., Tiran-Cappello, A., Cohen, C., Lardeux, S., George, O., Koob, G. F., Ahmed, S. H. & Baunez, C. Subthalamic nucleus high frequency stimulation prevents and reverses escalated cocaine use. *Mol. Psychiatry* 1 (2018). doi:10.1038/s41380-018-0080-y
46. Pelloux, Y. & Baunez, C. Deep brain stimulation for addiction: why the subthalamic nucleus should be favored. *Curr. Opin. Neurobiol.* **23**<bvertical-align:super;>,</bvertical-align:super;> 713–720 (2013).
47. Broen, M., Duits, A., Visser-Vandewalle, V., Temel, Y. & Winogrodzka, A. Impulse control and related disorders in Parkinson's disease patients treated with bilateral subthalamic nucleus stimulation: a review. *Parkinsonism Relat. Disord.* **17**<bvertical-align:super;>,</bvertical-align:super;> 413–417 (2011).
48. Benabid, A. L., Pollak, P., Louveau, A., Henry, S. & de Rougemont, J. Combined (thalamotomy and stimulation) stereotactic surgery of the VIM thalamic nucleus for bilateral Parkinson disease. *Appl. Neurophysiol.* **50**<bvertical-align:super;>,</bvertical-align:super;> 344–346 (1987).
49. Follett, K. A. The Surgical Treatment of Parkinson's Disease. *Annu. Rev. Med.* **51**<bvertical-align:super;>,</bvertical-align:super;> 135–147 (2000).

50. Lüscher, C. & Pollak, P. Optogenetically inspired deep brain stimulation: linking basic with clinical research. *Swiss Med. Wkly.* **146**<bvertical-align:super;>,</bvertical-align:super;> w14278 (2016).
51. Lim, S.-Y., O'Sullivan, S. S., Kotschet, K., Gallagher, D. A., Lacey, C., Lawrence, A. D., Lees, A. J., O'Sullivan, D. J., Peppard, R. F., Rodrigues, J. P., Schrag, A., Silberstein, P., Tisch, S. & Evans, A. H. Dopamine dysregulation syndrome, impulse control disorders and punding after deep brain stimulation surgery for Parkinson's disease. *J. Clin. Neurosci.* **16**<bvertical-align:super;>,</bvertical-align:super;> 1148–1152 (2009).
52. Pathological gambling after bilateral subthalamic nucleus stimulation in Parkinson disease | Journal of Neurology, Neurosurgery & Psychiatry. at <http://jnnp.bmj.com/content/78/5/517.short>
53. Brzosko, Z., Mierau, S. B. & Paulsen, O. Neuromodulation of Spike-Timing-Dependent Plasticity: Past, Present, and Future. *Neuron* **103**<bvertical-align:super;>,</bvertical-align:super;> 563–581 (2019).
54. Cui, Y., Prokin, I., Xu, H., Delord, B., Genet, S., Venance, L. & Berry, H. Endocannabinoid dynamics gate spike-timing dependent depression and potentiation. *eLife* **5**<bvertical-align:super;>,</bvertical-align:super;> e13185 (2016).
55. Gurney, K. N., Humphries, M. D. & Redgrave, P. A new framework for cortico-striatal plasticity: behavioural theory meets in vitro data at the reinforcement-action interface. *PLoS Biol.* **13**<bvertical-align:super;>,</bvertical-align:super;> e1002034 (2015).
56. Bi, G. & Poo, M. Synaptic Modifications in Cultured Hippocampal Neurons: Dependence on Spike Timing, Synaptic Strength, and Postsynaptic Cell Type. *J. Neurosci.* **18**<bvertical-align:super;>, </bvertical-align:super;> 10464–10472 (1998).
57. Sagot, B., Li, L. & Zhou, F.-M. Hyperactive Response of Direct Pathway Striatal Projection Neurons to L-dopa and D1 Agonism in Freely Moving Parkinsonian Mice. *Front. Neural Circuits* **12**<bvertical-align:super;>,</bvertical-align:super;> (2018).
58. Gulledge, A. T. & Stuart, G. J. Action Potential Initiation and Propagation in Layer 5 Pyramidal Neurons of the Rat Prefrontal Cortex: Absence of Dopamine Modulation. *J. Neurosci.* **23**<bvertical-align:super;>,</bvertical-align:super;> 11363–11372 (2003).
59. Kerr, J. N. D. & Plenz, D. Action Potential Timing Determines Dendritic Calcium during Striatal Up-States. *J. Neurosci.* **24**<bvertical-align:super;>,</bvertical-align:super;> 877–885 (2004).
60. Hjorth, J., Zilberter, M., Oliveira, R. F., Blackwell, K. T. & Hellgren Kotaleski, J. GABAergic control of backpropagating action potentials in striatal medium spiny neurons. *BMC Neurosci.* **9**<bvertical-align:super;>,</bvertical-align:super;> P105 (2008).
61. Kupchik, Y. M., Brown, R. M., Heinsbroek, J. A., Lobo, M. K., Schwartz, D. J. & Kalivas, P. W. Coding the direct/indirect pathways by D1 and D2 receptors is not valid for accumbens projections. *Nat. Neurosci.* **18**<bvertical-align:super;>,</bvertical-align:super;> 1230–1232 (2015).
62. Hwa, L. S., Chu, A., Levinson, S. A., Kayyali, T. M., DeBold, J. F. & Miczek, K. A. Persistent escalation of alcohol drinking in C57BL/6J mice with intermittent access to 20% ethanol. *Alcohol. Clin. Exp. Res.* **35**<bvertical-align:super;>,</bvertical-align:super;> 1938–1947 (2011).

63. Starski, P., Hong, S.-I., Peyton, L., Oliveros, A., Wininger, K., Hutchison, C., Kang, S., Karpyak, V. & Choi, D.-S. Ethanol induces maladaptive impulse control and decreased seeking behaviors in mice. *Addict. Biol.* **25**<bvertical-align:super;>,</bvertical-align:super;> e12754 (2020).
64. Rhodes, J. S., Best, K., Belknap, J. K., Finn, D. A. & Crabbe, J. C. Evaluation of a simple model of ethanol drinking to intoxication in C57BL/6J mice. *Physiol. Behav.* **84**<bvertical-align:super;>, </bvertical-align:super;> 53–63 (2005).
65. Lo, M.-C., Younk, R. & Widge, A. S. Paired Electrical Pulse Trains for Controlling Connectivity in Emotion-Related Brain Circuitry. *IEEE Trans. Neural Syst. Rehabil. Eng.* **28**<bvertical-align:super;>, </bvertical-align:super;> 2721–2730 (2020).
66. Huang, C. C. Y., Ma, T., Roltsch Hellard, E. A., Wang, X., Selvamani, A., Lu, J., Sohrabji, F. & Wang, J. Stroke triggers nigrostriatal plasticity and increases alcohol consumption in rats. *Sci. Rep.* **7**<bvertical-align:super;>,</bvertical-align:super;> 2501 (2017).
67. Wei, X., Ma, T., Cheng, Y., Huang, C. C. Y., Wang, X., Lu, J. & Wang, J. Dopamine D1 or D2 receptor-expressing neurons in the central nervous system. *Addict. Biol.* **23**<bvertical-align:super;>,</bvertical-align:super;> 569–584 (2018).
68. Fanelli, R. R. & Robinson, D. L. Dopamine D1 receptor blockade impairs alcohol seeking without reducing dorsal striatal activation to cues of alcohol availability. *Brain Behav.* **5**<bvertical-align:super;>,</bvertical-align:super;> (2015).
69. Boudkkazi, S., Carlier, E., Ankri, N., Caillard, O., Giraud, P., Fronzaroli-Molinieres, L. & Debanne, D. Release-Dependent Variations in Synaptic Latency: A Putative Code for Short- and Long-Term Synaptic Dynamics. *Neuron* **56**<bvertical-align:super;>,</bvertical-align:super;> 1048–1060 (2007).
70. Pawlak, V. & Kerr, J. N. D. Dopamine Receptor Activation Is Required for Corticostriatal Spike-Timing-Dependent Plasticity. *J. Neurosci.* **28**<bvertical-align:super;>,</bvertical-align:super;> 2435–2446 (2008).
71. Vignoud, G., Venance, L. & Touboul, J. D. Interplay of multiple pathways and activity-dependent rules in STDP. *PLoS Comput. Biol.* **14**<bvertical-align:super;>,</bvertical-align:super;> e1006184 (2018).
72. Fino, E., Glowinski, J. & Venance, L. Bidirectional Activity-Dependent Plasticity at Corticostriatal Synapses. *J. Neurosci.* **25**<bvertical-align:super;>,</bvertical-align:super;> 11279–11287 (2005).
73. Weiss, F., Parsons, L. H., Schulteis, G., Hyytiä, P., Lorang, M. T., Bloom, F. E. & Koob, G. F. Ethanol Self-Administration Restores Withdrawal-Associated Deficiencies in Accumbal Dopamine and 5-Hydroxytryptamine Release in Dependent Rats. *J. Neurosci.* **16**<bvertical-align:super;>,</bvertical-align:super;> 3474–3485 (1996).
74. Hirth, N., Meinhardt, M. W., Noori, H. R., Salgado, H., Torres-Ramirez, O., Uhrig, S., Broccoli, L., Vengeliene, V., Roßmanith, M., Perreau-Lenz, S., Köhr, G., Sommer, W. H., Spanagel, R. & Hansson, A. C. Convergent evidence from alcohol-dependent humans and rats for a hyperdopaminergic state in protracted abstinence. *Proc. Natl. Acad. Sci. U. S. A.* <bvertical-align:super;>113</bvertical-align:super;><bvertical-align:super;>,</bvertical-align:super;> 3024–3029 (2016).

75. Saunders, A., Oldenburg, I. A., Berezovskii, V. K., Johnson, C. A., Kingery, N. D., Elliott, H. L., Xie, T., Gerfen, C. R. & Sabatini, B. L. A direct GABAergic output from the basal ganglia to frontal cortex. *Nature* **521**<bvertical-align:super;>,</bvertical-align:super;> 85–89 (2015).

76. Xu, H., Perez, S., Cornil, A., Detraux, B., Prokin, I., Cui, Y., Degos, B., Berry, H., de Kerchove d'Exaerde, A. & Venance, L. Dopamine-endocannabinoid interactions mediate spike-timing-dependent potentiation in the striatum. *Nat. Commun.* **9**<bvertical-align:super;>,</bvertical-align:super;> 4118 (2018).

77. Creed, M., Pascoli, V. J. & Lüscher, C. Refining deep brain stimulation to emulate optogenetic treatment of synaptic pathology. *Science* **347**<bvertical-align:super;>,</bvertical-align:super;> 659–664 (2015).

78. Creed, M. Current and emerging neuromodulation therapies for addiction: insight from pre-clinical studies. *Curr. Opin. Neurobiol.* **49**<bvertical-align:super;>,</bvertical-align:super;> 168–174 (2018).

79. Kim, Y.-C., Alberico, S. L., Emmons, E. & Narayanan, N. S. New therapeutic strategies targeting D1-type dopamine receptors for neuropsychiatric disease. *Front. Biol.* **10**<bvertical-align:super;>,</bvertical-align:super;> 230–238 (2015).

80. R.S, L. R. S. LIII. On the character of the complete radiation at a given temperature. *Lond. Edinb. Dublin Philos. Mag. J. Sci.* **27**<bvertical-align:super;>,</bvertical-align:super;> 460–469 (1889).

81. Nespoli, E., Rizzo, F., Boeckers, T., Schulze, U. & Hengerer, B. Altered dopaminergic regulation of the dorsal striatum is able to induce tic-like movements in juvenile rats. *PLoS ONE* **13**<bvertical-align:super;>,</bvertical-align:super;> (2018).

82. Maia, T. V., Cooney, R. E. & Peterson, B. S. The Neural Bases of Obsessive-Compulsive Disorder in Children and Adults. *Dev. Psychopathol.* **20**<bvertical-align:super;>,</bvertical-align:super;> 1251–1283 (2008).

83. Kreitzer, A. C. & Malenka, R. C. Striatal Plasticity and Basal Ganglia Circuit Function. *Neuron* **60**<bvertical-align:super;>,</bvertical-align:super;> 543–554 (2008).

84. McCutcheon, R. A., Abi-Dargham, A. & Howes, O. D. Schizophrenia, Dopamine and the Striatum: From Biology to Symptoms. *Trends Neurosci.* **42**<bvertical-align:super;>,</bvertical-align:super;> 205–220 (2019).

85. Shen, W., Flajolet, M., Greengard, P. & Surmeier, D. J. Dichotomous Dopaminergic Control of Striatal Synaptic Plasticity. *Science* **321**<bvertical-align:super;>,</bvertical-align:super;> 848–851 (2008).

86. Parker, J. G., Marshall, J. D., Ahanonu, B., Wu, Y.-W., Kim, T. H., Grewe, B. F., Zhang, Y., Li, J. Z., Ding, J. B., Ehlers, M. D. & Schnitzer, M. J. Diametric neural ensemble dynamics in parkinsonian and dyskinetic states. *Nature* **557**<bvertical-align:super;>,</bvertical-align:super;> 177–182 (2018).

87. Kravitz, A. V., Freeze, B. S., Parker, P. R. L., Kay, K., Thwin, M. T., Deisseroth, K. & Kreitzer, A. C. Regulation of parkinsonian motor behaviours by optogenetic control of basal ganglia circuitry. *Nature* **466**<bvertical-align:super;>,</bvertical-align:super;> 622–626 (2010).

88. Lee, Y., Zhang, Y., Kim, S. & Han, K. Excitatory and inhibitory synaptic dysfunction in mania: an emerging hypothesis from animal model studies. *Exp. Mol. Med.* **50**<bvertical-align:super;>, </bvertical-align:super;> 1–11 (2018).

Figures

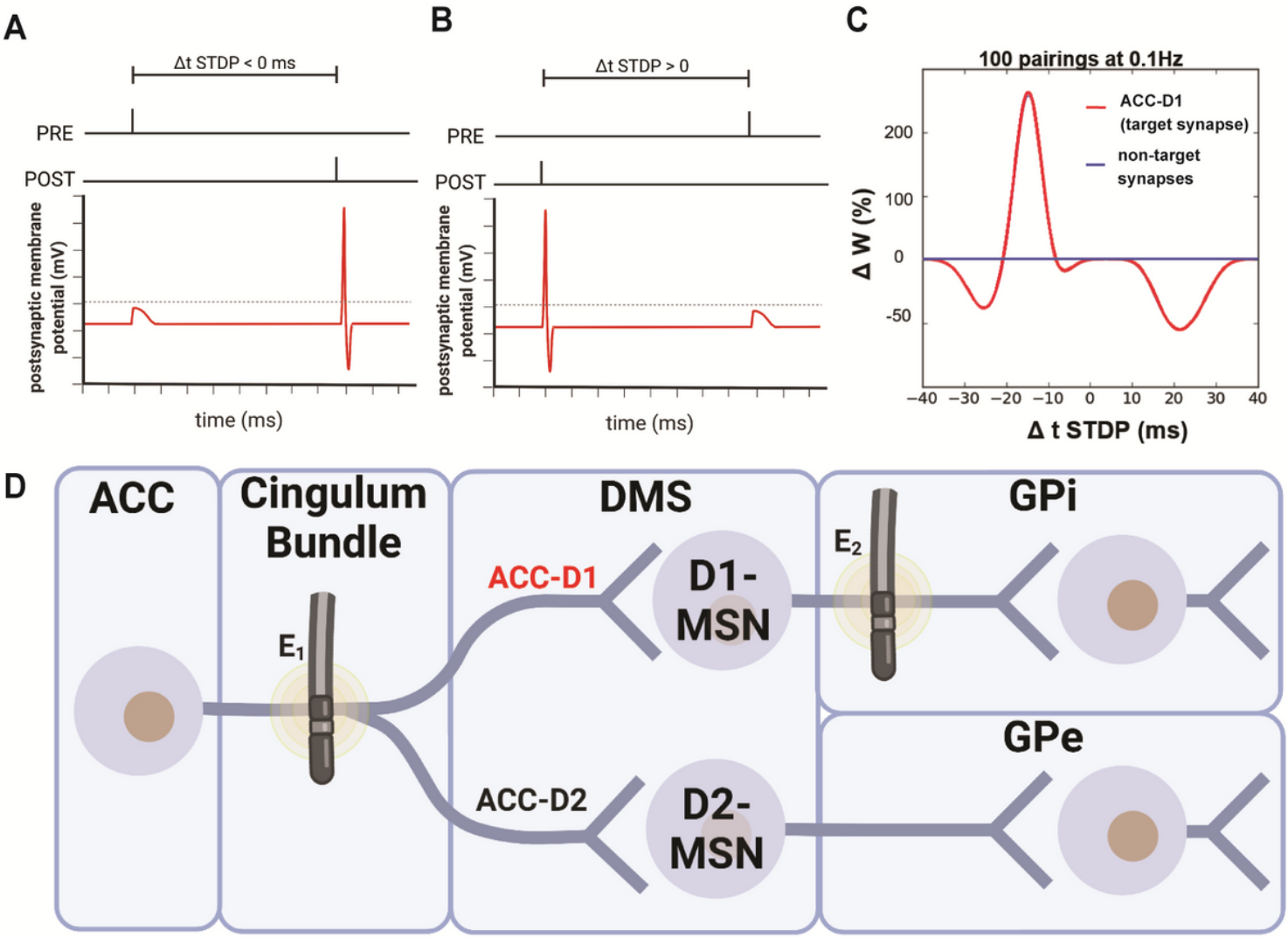

Figure 1

ULF-STDP(+/-) stimulation approach for bi-directional network gain control. **(A)** ULF-STDP(-) and **(B)** ULF-STDP(+) protocol schematics. **(C)** Biophysical model of STDP adapted from (Cui, et al., 2016)[56]. **(D)** Schematic representation of ULF-STDP protocol where an electrical stimulus is applied by electrode E_1 to cortical axons projecting from the ACC within a temporal window with respect to stimulation of postsynaptic axons of D1-MSN cells by electrode E_2. In this schematic, orthodromic action potential propagation from ACC axons paired with antidromic action potential propagation from D1-MSN axons in alters the gain of the spatially unique target synapse (ACC to D1-MSN) while gain of non-target synapses are unchanged. This protocol is repeated at £1Hz for 10 minutes. Abbreviations are as follows: Anterior cingulate cortex (ACC), dorsal medial striatum (DMS), medium spiny neuron (MSN), internal globus pallidus (GPi), external globus pallidus (GPe). Created with BioRender.com

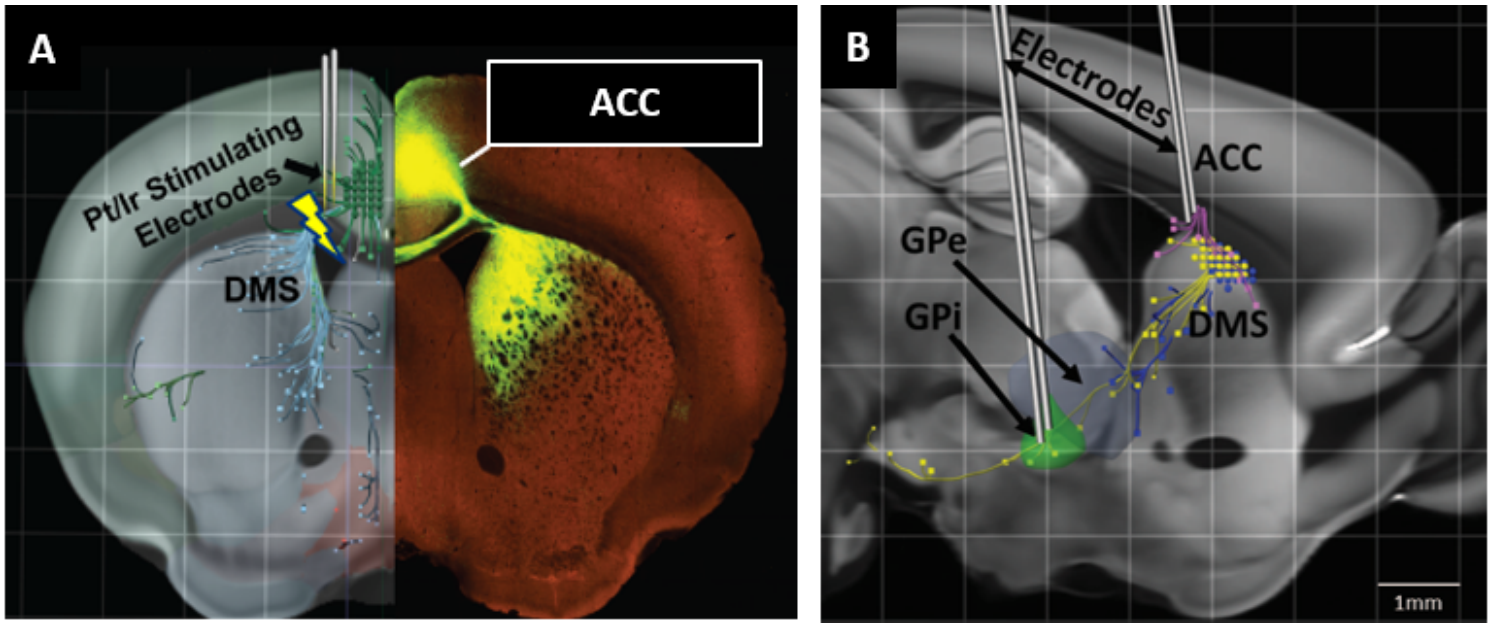

Figure 2

D1-MSN efferents are separable from D2-MSN efferents in GPi. (A) Probabilistic connectivity model (left hemisphere) of mouse histological tracer experiment (right hemisphere) showing efferents projecting to DMS labeled with eGFP. Electrodes are shown within axon bundle projecting from ACC to DMS. **(B)** D1-MSN efferents (yellow), can be targeted by placing a stimulating electrode in the GPi while avoiding D2-MSN efferents (blue). ACC efferents projecting to DMS (magenta) are targeted with an additional electrode. Data source: Allen Mouse Brain Connectivity Atlas (2011), experiments 159223001 and 127224133.

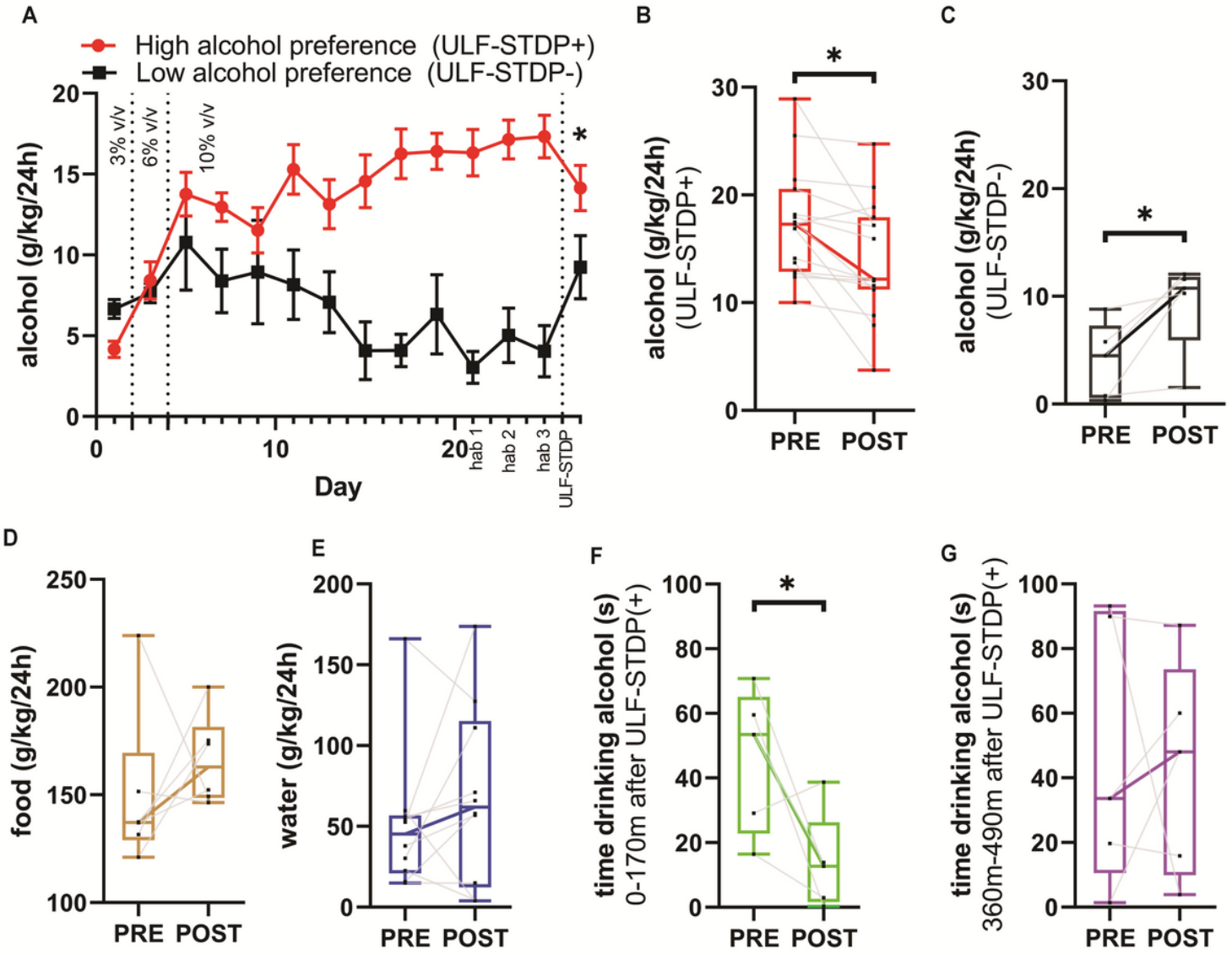

Figure 3

ULF-STDP allows bidirectional control of alcohol consumption in a two-bottle choice model of AUD without influencing other affective behaviors such as food and water consumption. **(A)** ULF-STDP(+) reduces alcohol consumption in mice displaying high alcohol preference, while ULF-STDP(-) increases alcohol consumption in mice displaying low alcohol preference. **(B)** Alcohol consumption in g/kg/24h period before ULF-STDP(+/-) (PRE) and 24 hours after ULF-STDP(+/-) (POST) for the ULF-STDP(+) and **(C)** ULF-STDP(-) protocols. **(D)** Food and **(E)** water consumption (g/kg/24h) in a random subset of the high alcohol preference group. **(F)** Time drinking alcohol as determined by an IR beam break sensor placed in front of the alcohol sipper for the first 170 minutes of the night cycle on the day before (PRE) and after (POST) ULF-STDP(+) and **(G)** 360-490 min of the night cycle on the day before (PRE) and after (POST) ULF-STDP(+). *PRE* indicates the 24 hours before ULF-STDP(+/-) and *POST* indicates the 24 hours after ULF-STDP(+/-). Statistical significance of comparison of alcohol consumption immediately before and after ULF-STDP was determined using Student's t-test, $p<0.05$ (n=15). Error bars represent standard

error. Box and whisker plots in B-G represent median, 95% CI, and max/minimum where black dots and gray lines represent individual animals.

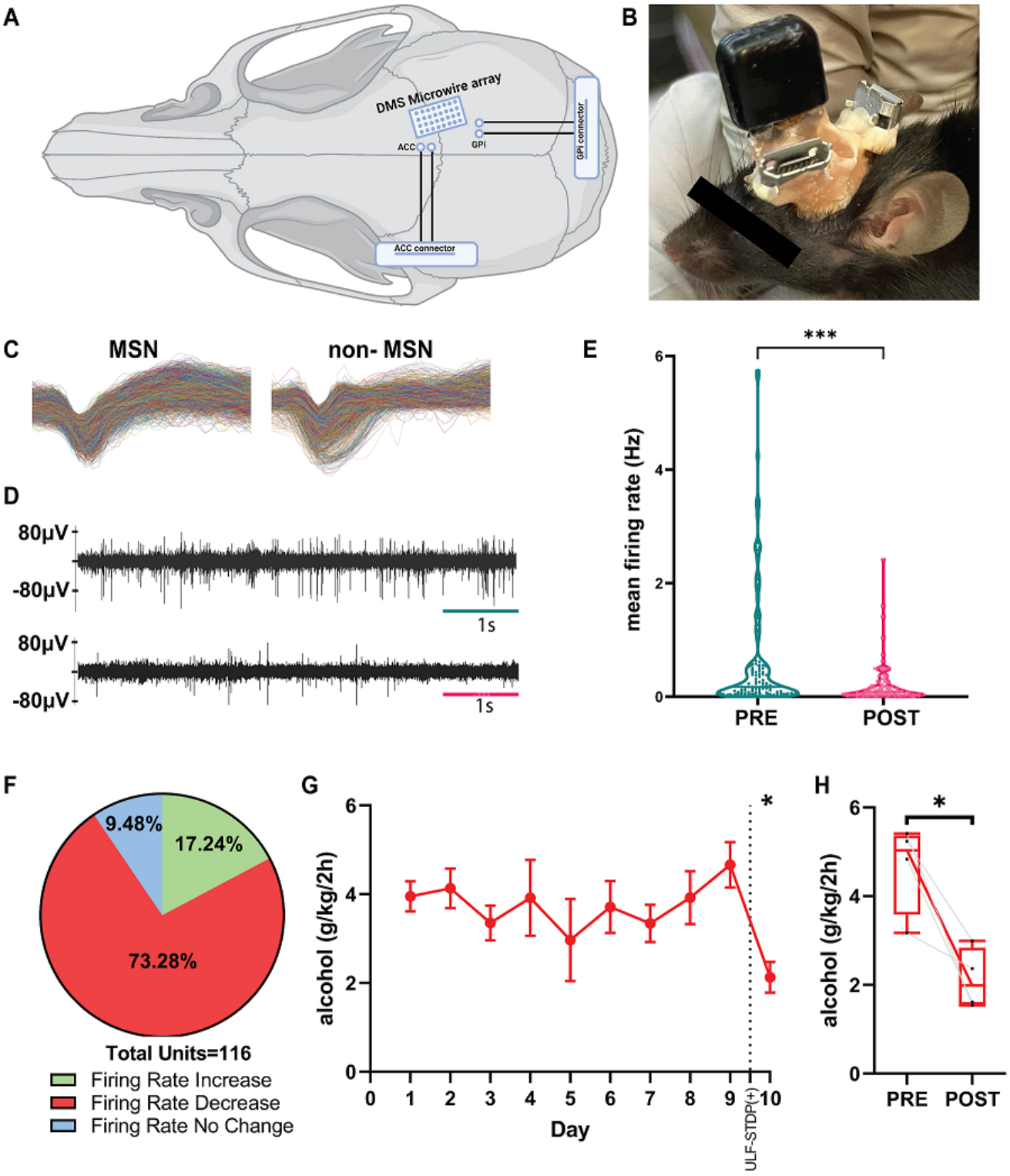

Figure 4

Electrophysiological DMS activity in AUD mice before and after ULF-STDP(+). (A) Schematic and **(B)** image of recording microwire array and stimulating electrode placement in the DMS, ACC, and GPi, respectively. **(C)** Representative MSN (left) and non-MSN (right). **(D)** Representative filtered traces from microwire array recordings in DMS of alcohol-exposed animals before (top) and after (bottom) ULF-STDP(+). **(E)** Mean firing rate of DMS MSNs from alcohol-exposed animals before and after ULF-STDP(+). **(F)** Distribution of units which show an increase greater than 10% (Firing Rate Increase), a decrease of less than than -10%, (Firing Rate Decrease), and all others (Firing Rate No Change) of mean firing rate comparing PRE to POST ULF-STDP(+). **(G)** Chronic intermittent access 2-hr daily alcohol self-administration with ULF-STDP(+) delivered on day 10. **(H)** Detailed view of day 9 and 10 as "PRE" and "POST", respectively. Statistical significance determined using two-tailed Mann-Whitney test, $p<0.05$. Box and whisker plots in (H) represent median, 95% CI, and max/minimum where black dots and gray lines represent individual animals. Data shown for n=116 cells; n=4 mice. **(A)** Created with BioRender.com

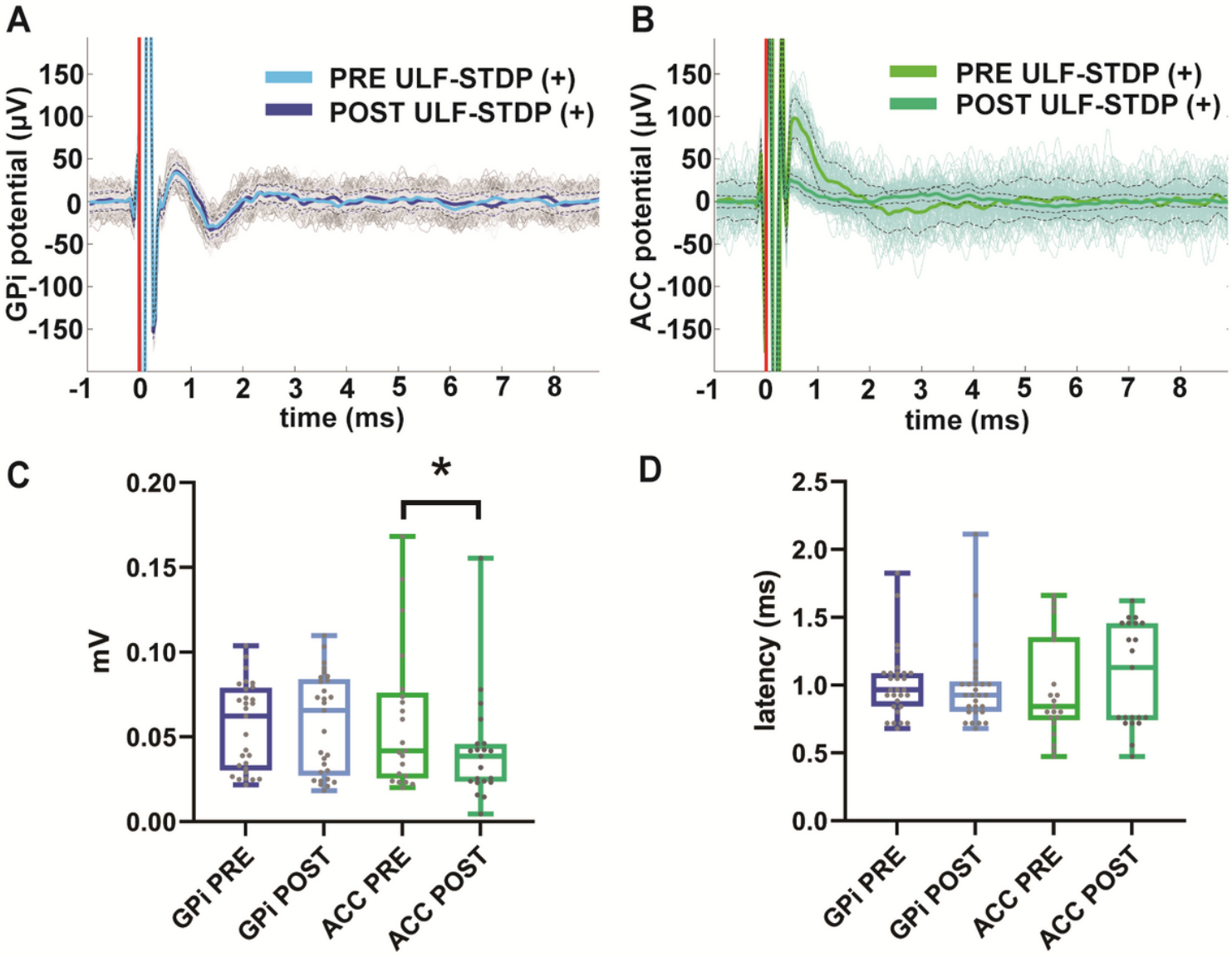

Figure 5

ULF-STDP(+) reduces evoked multi-unit potentials in DMS *in vivo.* **(A)** Example of acute microwire array recordings of multiunit responses evoked by stimulation of the GPi or **(B)** ACC stimulation before and after ULF-STDP(+). **(C)** Peak evoked amplitudes and **(D)** latencies to peak of evoked potentials are described. Statistical significance determined by paired Student's t-test (n=3 mice, n=21 channels, $p<0.05$).

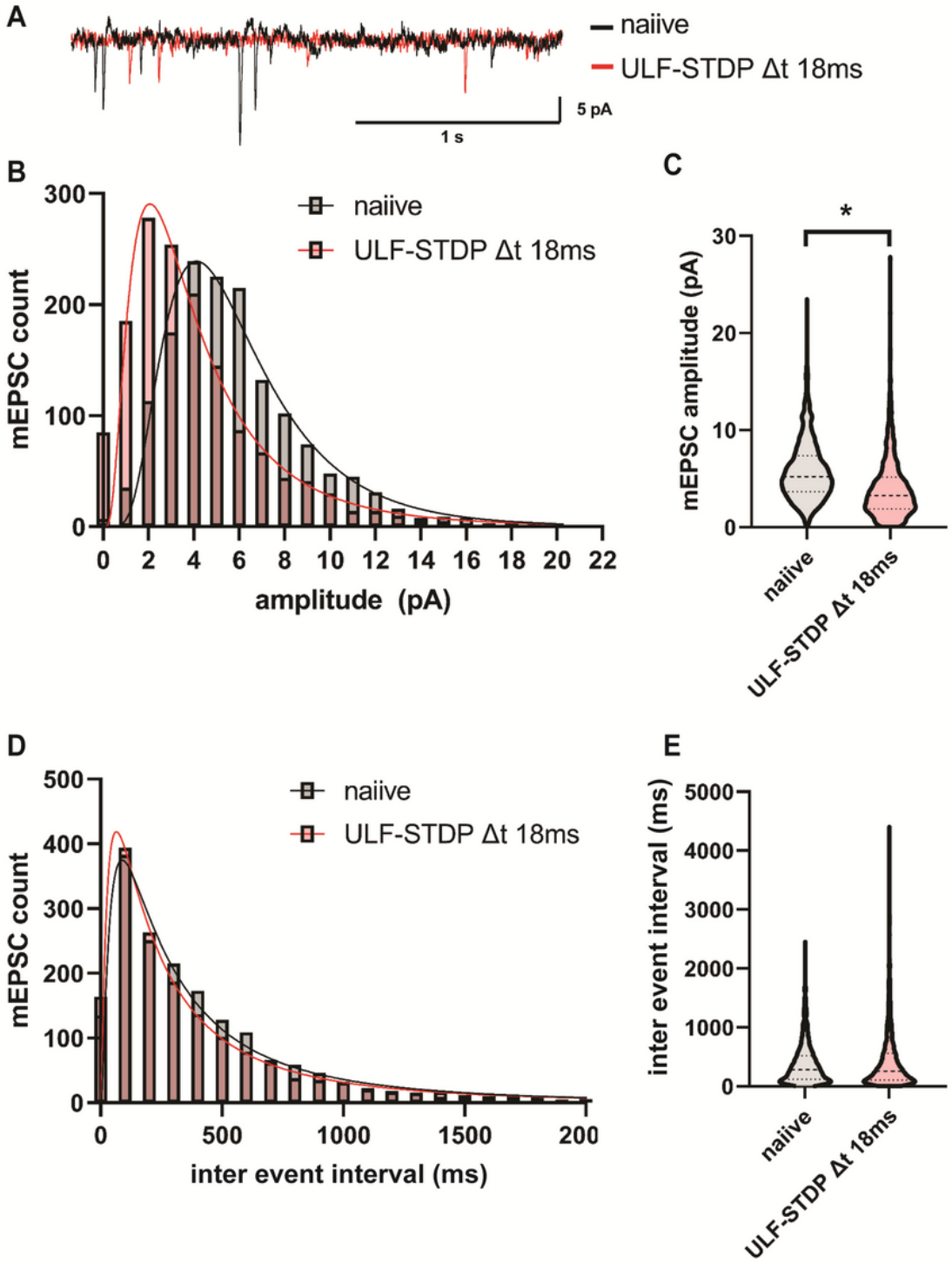

Figure 6

GPi/ACC ULF-STDP(+) decreases D1-MSN mEPSC amplitude, but not latency. (A) Example current traces from DMS D1-MSNs clamped at -75mV of naiive mice (black) and mice treated with ULF-STDP(+) *in vivo.* **(B)** Histogram showing mEPSC amplitude distribution and **(C)** violin plot of mEPSC amplitude**. (D)** Histogram showing mEPSC inter event interval distribution and **(E)** violin plot of mEPSC inter event

interval. Statistical significance determined by a two-tailed Mann-Whitney test (ULF-STDP(+) n=1 mouse, n=3 cells; naiive n=5 mice, n=1-3 cells/mouse, p<0.05)

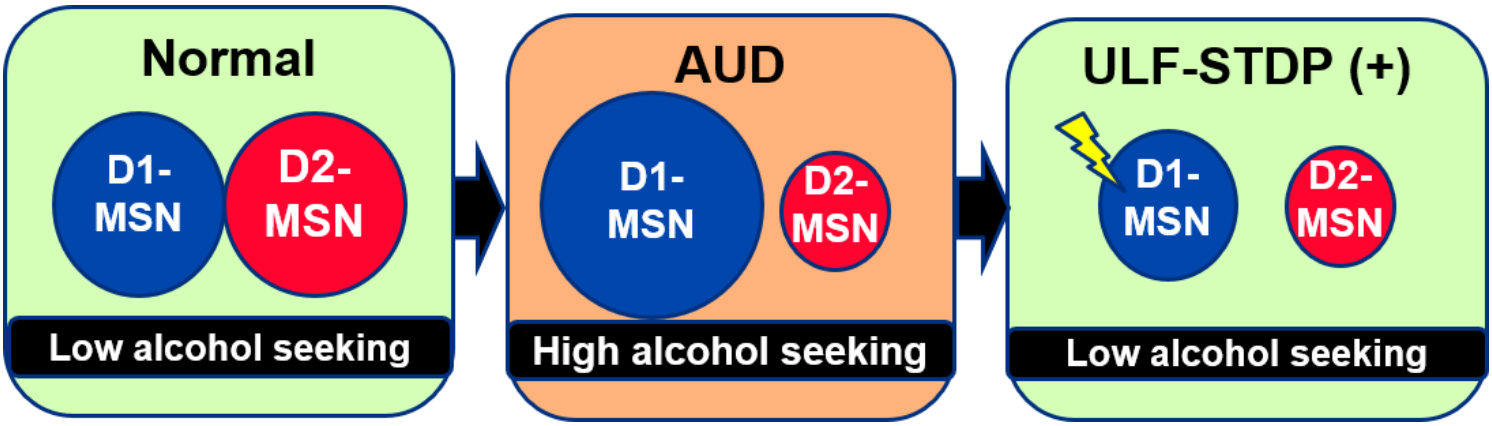

Figure 7

Schematic representation of the effects of ULF-STDP(+) on DMS D1-MSN hyperactivity and alcohol consumption. Circle size represents the strength of corticostriatal glutamatergic synapses.

Supplementary Files

This is a list of supplementary files associated with this preprint. Click to download.

- Aspetal.2022Supplementary.docx